Biodegradation Dynamics of Polymer–Starch Composites

R. P. WOOL,[1] D. RAGHAVAN,[2] G. C. WAGNER,[3] S. BILLIEUX[3]

[1] Department of Chemical Engineering and Center for Composite Materials, University of Delaware, Newark, Delaware 19716

[2] Department of Chemistry, Howard University, 525 College Street, NW, Washington, DC 20059

[3] Department of Materials Science and Engineering, University of Illinois, 1304 W. Green Street, Urbana, Illinois 61801

Received 8 July 1998; accepted 13 May 1999

ABSTRACT: The dynamics of starch biodegradation in polyethylene–starch (PE–S) composites was investigated by aerobic biodegradation methods and computer simulations, with the starch fraction p above and below the percolation threshold p_c. Two models for starch degradation were considered: (i) microbial invasion through the composite and (ii) macromolecular (enzyme) diffusion which results in the back-diffusion of small molecules to the surface for further assimilation by microorganisms. The microbial-invasion model was based on scanning electron microscopy (SEM) studies of PE–S composites that contained a 1–15-micron distribution of starch particles. Following exposure to soil test conditions, micrographs of thin films clearly showed the colonization of microorganisms within channels of the matrix that were initially occupied by starch. The enzymatic diffusion was based on hydrolytic experiments of PE–S composites. Following exposure of a composite to a hydrolytic test condition, small molecules were produced. The starch accessed by microbes and enzymes was computed by simulating degradation of a monodisperse and polydisperse (starch grains of 1–10-micron diameter) composite. Aerobic degradation studies in a biometer indicate that the starch accessibility. A follows a power-law dependence with time $A \sim t^n$, where the exponent n depends on the fractal dimension of the accessed starch clusters and pathways and approaches unity when $p > p_c$. Microbial invasion simulations indicate that the average power-law exponent near p_c is approximately 0.5 and approaches 1.0 at $p > pc$, whereas the enzymatic diffusion simulations indicate that the average power-law exponent near p_c is about 0.25 and approaches 0.5 at $p > pc$. The observed exponent for the aerobic degradation study suggests that for composites with a starch fraction less than and greater than p_c the starch is predominantly accessed by microbial invasion. © 2000 John Wiley & Sons, Inc. J Appl Polym Sci 77: 1643–1657, 2000

Key words: biodeuradable, plastic, pereolation polymer-starch composites, dynamics

INTRODUCTION

There are four synergistic mechanisms by which plastic materials degrade in aquatic and terrestrial environments.[1–4] The degradation mechanisms are as follows:

1. *Microbial degradation,* where fungi and bacteria-secreting enzymes degrade the plastic under aerobic or anaerobic conditions. The rate of degradation is sensitive to microbial population, moisture, temperature, and oxygen in the environment. Plastics (such as poly(hydroxy buterate valerate) (PHBV), poly(vinyl alcohol)

Correspondence to: R. P. Wool.

Contract grant sponsor: National Science Foundation; contract grant number: 9596-267.

Contract grant sponsor: State of Illinois, Office of Solid Waste Research; IBM Corp.

Journal of Applied Polymer Science, Vol. 77, 1643–1657 (2000)

(PVOH), and polycaprolactone (PCL, starch-, cellulose-, and triglyceride-based plastics) which degrade by this mechanism are expected to be termed biodegradable. Plastics which are invaded by microbes are also susceptible to macroorganism degradation.[5]

2. *Macroorganism degradation,* where invertebrates and insects such as crickets, slugs, and snails consume the plastic as food. Fish and large animals also consume plastics, often causing themselves great bodily harm. Macroorganism degradation occurs in three stages involving[1,4] (a) mastication, (b) digestion, and (c) exocorporeal degradation. Mastication (chewing) results in considerable deterioration of the physical and chemical structure of the plastic; digestion in the macroorganism removes the digestible components by enzymes and mechanochemical action; exocorporeal degradation involves the fate of nondigested fecal material and orally contacted pieces of plastic. Comparatively little research has been done in this area, even through it is typically the fastest mechanism of degradation. Plastics which are nonbiodegradable can still be made degradable by this mechanism by being attractive to macroorganisms via the incorporation of feeding stimulants.[2] Alternatively, one can add feeding retardants which discourage attack by macroorganisms.
3. *Photodegradation,* where absorption of ultraviolet (UV) radiation from the sun leads to decomposition of the plastic molecules. This is a highly studied degradation process and, typically, commodity plastics [e.g., polyethylene (PE), polypropylene, polystyrene] contain additives to prevent them from degrading in sunlight. Photodegradation may be enhanced by the incorporation of photoactive chemical groups into a polymer chain (vinyl ketones and carbon monoxide) or by photoactive additives. Photodegradation has the potential of facilitating biodegradation by reducing the molecular weight and introducing oxygen groups on the chain, which also facilitates chemical degradation.
4. *Chemical degradation,* where chemical additives such as oxidants and peroxides promote reactions which lead to the deterioration of the plastic molecular structure. In such cases, catalyzed oxidation of double bonds (e.g., from unsaturated fats, oils, and low molecular weight rubber) produce peroxides which decompose into highly active free radicals. The latter have the potential to attack the polymer chains if they are not deactivated by other chemical species. This and other photochemical additives have been used primarily in PE to reduce molecular weight and cause embrittlement. Extensive reduction of molecular weight (ca. 1000) may result in some biodegradation.

Other factors such as mechanical action, wind, and rain can deteriorate the polymer. The extent to which polymers degrade is dependent on the environment surrounding the disposed polymer and type of polymer. It is well documented that hydrocarbon polymers such as PE and polystyrene, of $M_n > 100{,}000$, do not biodegrade within a realistic period of time (10 years).[6,7] The size of the individual polymer chains, the crystallinity, the chemical nature, and the branching points are some of the factors which influence the biodegradation of polymers.[7,8]

During the last 25 years, considerable interest has been expressed in substituting the traditional nondegradable polymers like PE by a biodegradable polymer like starch or poly(hydroxy butyrate valerate), especially for short-term applications without significantly sacrificing the mechanical properties of synthetic polymers.[9–11] Microbes create pores on consumption of the biopolymer and thereby increase the surface area of the composite.[12] It is believed that increased surface area may enhance oxygen-based reactions which could increase PE chain oxidation. Creating oxidized PE chain ends in a degraded polyethylene–starch (PE–S) composite will make PE susceptible to biotic reactions.

It is well documented that growth of microorganisms occurs on many polymers, especially when certain fillers or plasticizers are used in the polymer formulations.[13,14] Due to the microbial growth, polymers have been found to discolor. This surface growth resulting in the typical mold or darkened appearance may not result in degradation of the body of the polymer if confined to the surface. In the present study, we investigated the dynamics of microbial invasion and enzyme diffusion through model starch-filled PE composites. The design of a biodegradable composite with a predetermined lifetime is essential for many practical applications such as agricultural mulch films, compostable materials, degradable escape hatches for lobster pots, nursery pots, and fores-

tation planting. The lifetime of starch particles in an aerobic environment may be hours, but when placed in a nondegradable PE matrix, its lifetime increases from days to years, depending on the starch fraction and connectivity between particles. When the starch fraction exceeds the percolation threshold, significant pathways for microbial invasion are generated and degradation is accelerated.[12,15] In this article, we examined the kinetics of starch accessibility in PE–S composites, above and below the percolation threshold, by comparing the simulated kinetic results for microbial and enzymatic attack with aerobic biometer results. The results of this article are intended to provide a fundamental understanding of the kinetic aspects of biodegradation and assist in the design of more reliable biodegradable plastic and composite materials.

PERCOLATION THEORY

Scalar percolation theory deals with the connectivity of one component randomly dispersed in another.[16–19] Examples of percolation are gelation during crosslinking polymerization and conductivity of metal particles dispersed in a nonconducting medium.[18,19] The percolation threshold p_c for a finite-sized object is defined as the minimum concentration p (of the percolating medium) at which the contact of the bottom surface to the top surface is established. The percolation threshold p_c is different for lattices of different geometry.[16] For two-dimensional site percolation, the threshold p_c is 59.40%, while p_c is 31.17% for a cubic lattice. Other important forms of percolation are gradient percolation,[20] where the concentration of particles p is not constant (often encountered in polymer films), and vector percolation,[21] where one examines the propagation of forces or vectors through the composite. Vector percolation is important in determining mechanical properties, especially the fracture stress.[22,23] Examples and further descriptions of scalar, gradient, and vector percolation are given in Chapter 4 of ref. 22. In this article, we confine our analysis and discussion to scalar percolation in two and three dimensions.

Peanasky et al. applied the scalar percolation theory to analyze the static degradation of starch in PE–S composites.[12] In this case, static degradation is determined by the final accessibility of starch or the total starch concentration that can be accessed by microorganisms. This model does not consider the time aspect of degradation. Simulations relating to static degradation were discussed in an earlier publication.[2,12] The fraction accessed as a function of concentration $A(p)$ is determined by the percolation relation:

$$A(p) \sim (p - p_c)^v/p \qquad (p > p_c) \tag{1}$$

where p_c is the critical percolation concentration or percolation threshold, and v, the critical exponent. Figure 1 shows the accessed fraction (dark) cluster for bilater invasion in two dimensions near the percolation threshold.[12] The exponents for three-dimensional PE–S systems were computed by Peanasky et al.[12] using $v = 0.41$ and $p_c = 0.3117$. Typically, in three dimensions, eq. (1) is valid in the range of p values of $0.3117 < p < 0.35$.

Equation (1) describes $A(p)$ in the vicinity of p_c for an infinitely large sample, such that when $p < p_c$, $A(p) = 0$. However, for real polymer materials, especially films, $A(p)$ is not zero when $p < p_c$ since clusters of starch can be accessed from the surface, as shown in Figure 1(a). In this case, Wool[22,24] showed that the accessed fraction f can be described by the relation

$$f = 2(b/h)|1 - p/p_c|^{-\alpha} \qquad (p < p_c) \tag{2}$$

where b is the particle diameter, h is the thickness of the sample, and α is determined by

$$\alpha = v(D - d + 1) \tag{3}$$

in which D is the fractal dimension of the clusters; d, the dimension of the sample (typically $d = 2$ or 3); and v, the cluster correlation exponent. In three dimensions, $v = 0.8$, $D \sim 2.5$, and $\alpha \sim 0.4$; in two dimensions, $v = 4/3$, $D \sim 7/4$, and $\alpha \sim 1$. The factor of 2 in eq. (2) refers to the two exposed surfaces of the thin material and becomes unity if only one surface is exposed to degradation. In Figure 1(a), the surface accessibility is determined from eq. (2) using $p = 0.58$, $pc = 0.5927$, $b = 1$, $h = 512$, and $\alpha = 1$, as $f \sim 18\%$, which is in close agreement with this simulation ($\sim 17\%$).

The average cluster size ζ at $p < p_c$ is determined by

$$\zeta = b|p - p_c|^{-v} \tag{4}$$

Since this is a measure of the cluster size near the surface, it is an excellent method to determine the degraded or invaded depth. When the cluster size

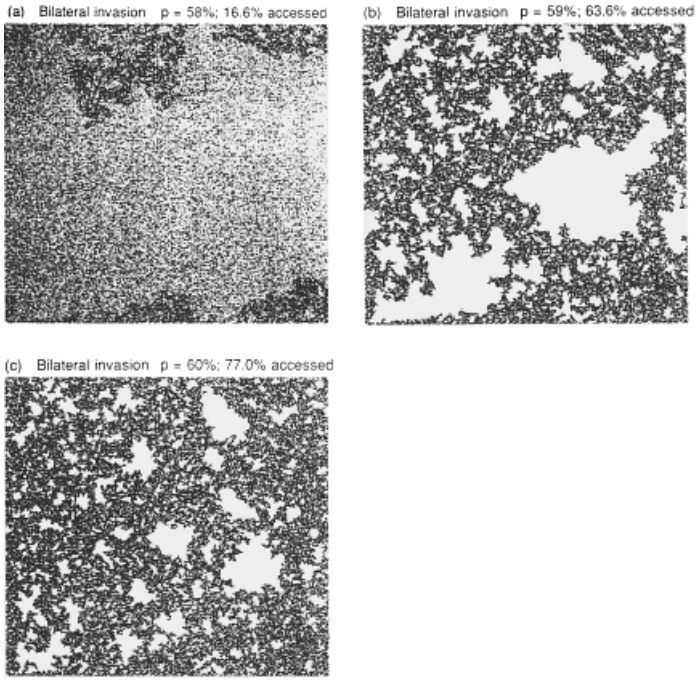

Figure 1 Effect of starch concentration on accessibility modeled by bilateral invasion from both the top and bottom sides. The square 512 × 512 lattice has occupation probabilities of (a) 58%, (b) 59%, and (c) 60%. Accessibilities are displayed for each panel.

exceeds the sample thickness, one obtains local percolation "holes" or localized percolation pathways, which is an interesting thin-film effect. The latter effect can also be used in the design of membranes with controlled porosity.

The above scalar percolation analyses refers to accessibility of starch where the starch concentration p is constant throughout the material. However, it often happens that a concentration gradient $p(x)$ can occur and this presents a very interesting situation which is treated by gradient percolation.[20] A concentration depth profile $p(x)$ varies smoothly as a function of the one-dimensional depth variable, x. However, when viewed in two or three dimensions, the profile or diffusion front is not smooth and can be very rough. The random nature of diffusion permits the formation of complex structures with fractal characteristics. The diffusion field in each case is divided into two parts: (1) a connected region which is accessible from the surface at $x = 0$, and (2) a nonconnected region at lower concentration which is embedded in the polymer matrix. The part nearest the surface, $p(0) = 1$, is connected to itself through a percolation criterion and the nonconnected part involves small clusters of particles which are not connected to the surface. The frontier separating the connected from the nonconnected regions is called the "diffusion front" by Sapoval et al.[20] The diffusion front has fractal character and provides an elegant method of describing the naturally rough structure of the connected/nonconnected interface. The position of the front X_c occurs at the position of the scalar percolation threshold p_c in the concentration gradient.

The roughness and position of the diffusion front X_c varies as a function of the diffusion length L_d. For a linear concentration gradient in three dimensions, the number of accessible particles is determined as a function of L_d by $A(L_d) = 1.3\ L_d$. The latter relation is derived from the integral between 0 and X_c in the concentration profile, $p(x) = 1 - x/3L_d$, with $X_c \approx 2\ L_d$. Since the volume associated with $A(L_d)$ is proportional to X_c, the accessed fraction $A = 0.65$ is constant for a linear concentration gradient. Similar behavior is observed for all monotonically decreasing depth profiles. However, the affected degraded depth can be significant and is determined by $X_c \sim L_d$. A detailed analysis of gradient percolation for polymer interfaces is available.[22]

In the current topic, we extend the percolation theory to investigate the dynamic degradation $A(t)$ of starch in PE–S composites with respect to

the concentration p, invasion mechanism, microbial population, and starch size distribution. We first examine computer simulations of microbial invasion on percolating networks and then compare results with experiments and analysis.

COMPUTER SIMULATIONS

Microbial and Biochemical Considerations

The nature of microbial degradation of starch in a PE–S composite was investigated by computer simulation. *E. coli* was used as a model microbial species in the simulation because the cell physiology is well understood.[25] The mobility, efficiency of conversion of starch to carbon dioxide, the lifetime, and the reproduction rate of *E. coli* are well documented. The simulation was performed by allowing *E. coli,* the test microorganism, to invade the monodisperse (starch grains of 1-micron diameter) PE–S composite. During the simulation, the location of the microbial front in the composite was periodically profiled. While the initial runs were related to the unilateral invasion model (degradation occurs from either the top or the bottom surface), the starch is typically accessed by bilateral microbial invasion (degradation occurs from the top as well as the bottom surfaces). Peanasky et al.'s[12] studies indicated that the accessibility results obtained from bilateral invasion differ from those obtained using unilateral invasion, especially when the concentration of starch is below p_c. Therefore, the unilateral invasion model was refined to include the bilateral accessibility of starch as well as the polydisperse nature of the starch grains (starch grain diameter size distribution).

It was also reported in the literature that, following the exposure of the PE–S composite to enzymatic/acid test conditions, hydrolysis of starch grains result in the diffusion of the small molecules (glucose) to the polymer/microbe interface.[5,12] Starch is a copolymer of amylose and amylopectin and has glycosidic bonds. Enzymatic hydrolysis of starch involves the cleavage of glycosidic bonds in the presence of water. Monosaccharide, disaccharide, and oligomers of saccharide are formed during the process as a result of degradation. It is well documented that hydrolysis of starch eventually results in glucose. The enzyme-release rate, enzyme diffusion coefficient, and diffusion coefficient of the product (glucose) are documented and these were the parameters required for simulation. Simulations were performed by allowing the bilateral diffusion of enzymes through the monodisperse and polydisperse PE–S composites.

The dynamics of the invasion by microbes and enzymes were simulated in two dimensions using an 80×400 lattice on which the starch particles were placed with a probability p. The dimensions of the simulated matrix were similar to the dimensions of the experimental test material (aerobic and soil studies) in which the starch particle diameter-to-thickness ratio was $b/h \sim 10$. Composites above and below the percolation threshold ($p_c = 0.59$) were prepared in which the concentration of starch, p, in the samples ranged from 57 to 61%.

Simulation of Microbial Invasion

A 1-micron particle of starch was determined to contain 53 femtomoles (fmol) of carbon. The structure of an average microbe was calculated to contain 10.5 fmol of carbon. The carbon content of an average microbe was obtained by considering it to be $\sim$ 33% bigger than a young microbe. On attaining 14 fmol, the growing microbe divided into two new microbes, each with a carbon concentration of 7 fmol. The generation time of a microbe was determined to be 2400 s. It was assumed that microbes, on accessing 1-micron starch, could utilize approximately 39% as CO_2, 1% as fuel for motion, and the remainder as biomass. The microbial motion is dependent on the fuel content: In the absence of any starch, the microbe obtains its fuel by utilizing the carbon of its own microbial structure until the structure reaches a carbon concentration of 7 fmol. The average speed of microbial locomotion was assumed to be 1 cm/s.

A 10-micron layer of water with a 10% microbial concentration was placed in contact with the edge of the PE–S two-dimensional lattice. Once the lattice sites were visited and identified as occupied/unoccupied and the microbial parameters were defined, the simulation was initiated. Periodically, after 100 s, the lattice sites were sampled for the amount of starch accessed. The fraction of starch removed from the PE–S composite was plotted as a function of time.

Simulation of Enzymatic Diffusion

A diffusion-dependent enzyme-digestion model was investigated. An amylase enzyme concentration ($1M$) was placed on two edges of the lattice and simulated a breakdown of starch by an extracellular enzyme. The diffusion coefficient of the

enzymes and degradation product was 7.48 $\times 10^{-7}$ and 45.86 $\times 10^{-7}$ cm^2/s, respectively. The amount of starch accessed by the diffusing enzyme was plotted as a function of time.

EXPERIMENTAL

Materials Preparation

Corn starch supplied by Cargill Inc. Minneapolis MN, was uniformly mixed with low-density polyethylene (LDPE) supplied by Quantum Chemical Co. Cincinnatti OH, to form a PE–S composite. The concentration of starch ranged from 20 to 40% (by volume). The melt blending was achieved in a Brabender Data Processing Plasti-Corder Model PL2000 with a 350-cc capacity mixing-head attachment. The composites were then removed from the processing unit and compression-molded into plates of 100-micron thickness using a Carver Laboratory Press, Model M25.

Soil Test

Three inches of sifted soil was placed in a plastic box, 15 $\times$ 10 $\times$ 6.5 in., which was then lined with a stainless-steel cloth for air passage. Soil was kept moistened at a 30% content with deionized water.[15,26] Thin films of the PE–S composite (20–40% starch volume), 100 microns in thickness, were buried at a depth of 2 in. Samples were retrieved periodically for SEM study. The experiments were done in a room at ambient temperature (21–25°C) and humidity (37–90%).

Fracture surfaces of the degraded PE–S samples were prepared by immersing the composite in liquid nitrogen for 2 h. The samples were gently removed and cracked so as to obtain a brittle fracture surface. SEM micrographs of the fractured surface of the composites were taken using a Hitachi 600 SEM. The fracture surface of the composites before soil burial was also examined by SEM.

Aerobic Biodegradation Test

The essential features of the aerobic biodegradation test are as follows:

(i) Design of the biometer unit which consists of a scrubbing unit (CO_2 removal gas train), a production chamber for the composite (CO_2-producing main chamber), and a trapping unit (terminal gas chamber);
(ii) Standardization of the inoculum;
(iii) Biodegradation analysis of the polymer; and
(iv) Carbon balance of the polymer. Biodegradation involves complex biochemical mechanisms whereby the starch in the PE–S composite is broken down by microbial action. We assume that no biodegradation of PE occurs.

Biometer Design

The design of the biometer unit and the performance of the unit were described in detail elsewhere.[27–29]

Standardization of the Inoculum

The sludge material used as the microbial inoculum was procured from a waste-treatment plant and subjected to a two-step preparatory procedure. To achieve standardization of the inoculum, the residual organic matter from the inoculum was "oxidized" and removed before it was introduced in the biometer so that the carbon from the inoculum did not contribute to the degradation of the polymer. In the first step, standardization of the inoculum was achieved. Thirty milliliters of the sludge material was transferred to a 250-mL flask containing 21 mL of the nutrient medium and 50 mL of deionized water.[28,29] The solution was agitated at 1000 rpm using a magnetic stirrer. The growth of microbes was monitored spectrophotometrically using turbidity measurements, where the optical density of solutions containing a known microbe content was determined as a function of microbial content.[27] Using a light-scattering photometer (Model Spectronic 20), the optical density of the solution at 660 nm was recorded at periodic intervals from which the microbial concentration was determined.

Once the inoculum attained the stationary-growth phase, the sludge was transferred to a generic substrate. By allowing the sludge to grow on a generic substrate to a particular cell density, the standardized inoculum of optical density (OD) $OD_{660} \sim 2$ was obtained. In the second step, 10 mmol of glucose was added to the inoculum. The growth of the microbes was monitored spectrophotometrically. The glucose-adapted inoculum served as the inoculum for degradation studies on starch and the PE–S composites.

Biodegradation Analysis of PE–S Composites

The glucose-adapted microorganisms were further adapted to starch prior to serving as the

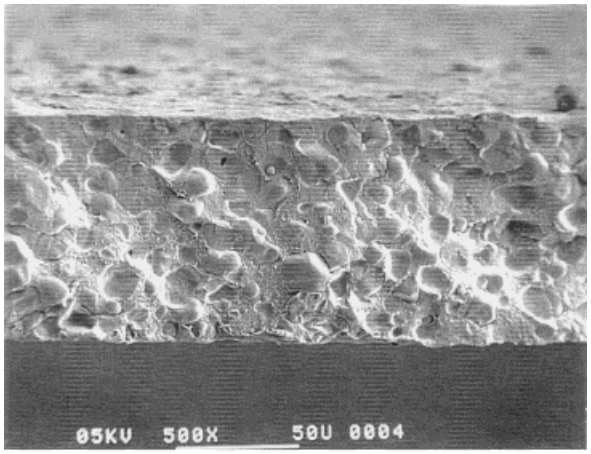

(a)

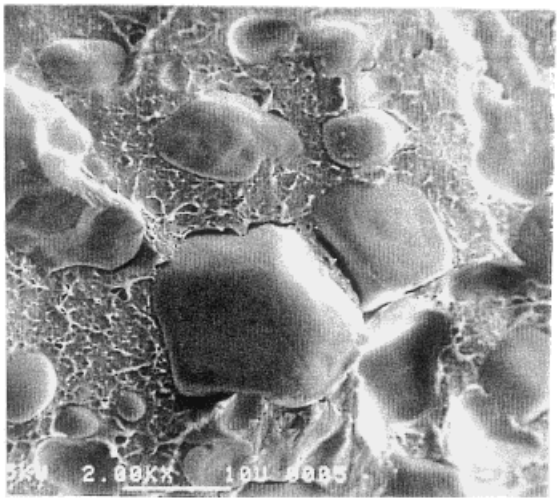

(b)

Figure 2 Micrograph of the fractured surface of an undegraded PE–S composite where starch is 40% by volume: (a) 500×; (b) 2000×.

inoculum for degradation studies on the PE–S composites. The starch-adapted inoculum (250 mL) was transferred to a stripping unit containing 1725 mL of deionized water and 525 mL of nutrient medium. By purging CO_2 free air through the inoculum for 12 h, the residual starch from the inoculum was oxidized. Then, the biometer unit was loaded with 1.5 g of the test material.

Five sets of biodegradation experiments were conducted: (i) with 100% starch, (ii) with 45–55 vol % PE–S composites, (iii) with 65–35 vol % PE–S composites, (iv) with 80–20 vol % PE–S composites, and (v) without test material. The experimental conditions were described in detail elsewhere.[29] At periodic time intervals, a carbon-balance experiment was conducted by withdraw-

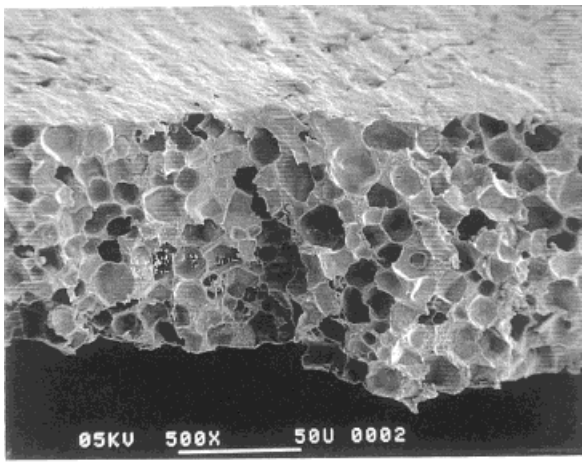

(a)

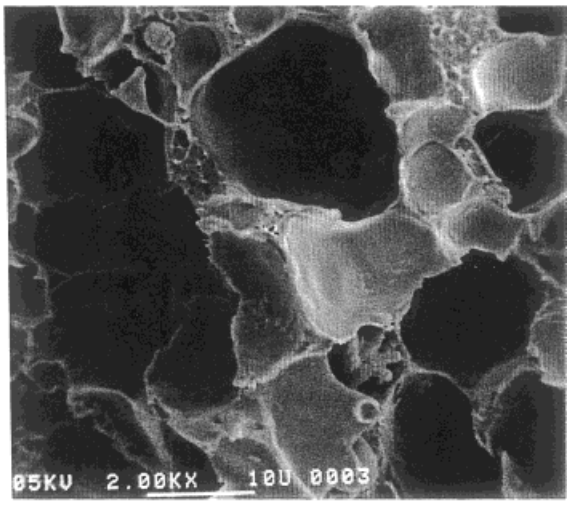

(b)

Figure 3 Micrograph of the fractured surface of a degraded PE–S composite where starch is 40% by volume: (a) 500×; (b) 2000×.

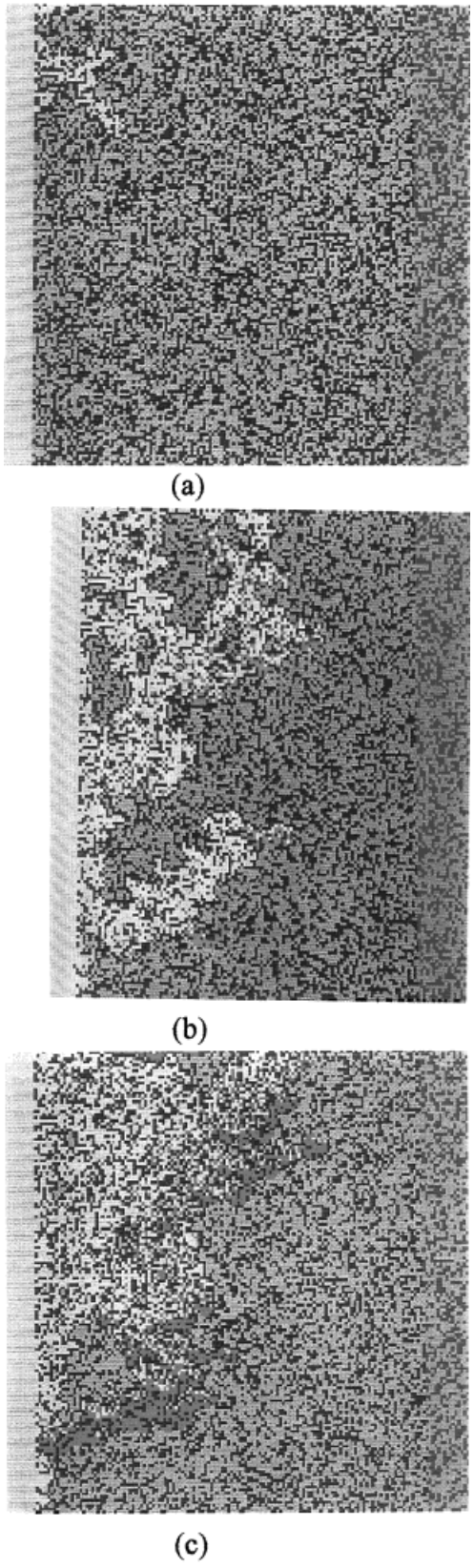

Figure 4 Effect of concentration on accessibility modeled by unilateral microbial invasion after a fixed time interval. The square 400 × 400 lattice has occupation probabilities of (a) 57%, (b) 59%, and (c) 61% for a monodisperse PE–S composite. Connectivities are displayed for each panel.

ing aliquots of liquid suspension, as described in the next section.

Carbon Balance Experiment

Assay of Gaseous (CO_2). The CO_2 produced by biodegradation of starch was removed by purging the reactor with CO_2-free air and collecting in a trap containing 125 g of 0.1 m NaOH solution. The amount of CO_2 was quantified by periodically assaying the decrease in alkalinity of the trap solution as follows: To the CO_2 trap, 12.5 g of 1 m NaOH solution was added. A 25-g aliquot was removed from the total 137.5 g and was titrated with HCl acid to a phenolphthalein end point (pH 7–8). Similarly, 25 g of the aliquot was weighed and 2.5 mL of a saturated barium chloride solution (1.6*M*) was added and titrated with HCl acid to a bromocresol green end point (pH 3–4). The difference between the readings corresponds to the amount of CO_2 collected in the trap.

Assay of Biomass and Soluble Carbon. During the biodegradation experiments of the PE–S composites, agitation of the biometer reactors was temporarily halted, to allow solid particles to form sediment. An aliquot of the liquid phase was withdrawn from the degradation chamber to record the OD of the solutions at a wavelength of 660 nm from which the microbial population and carbon in the biomass was determined. At the end of each experiment, the soluble carbon assay was also conducted to determine the dissolved polymeric carbon in solution.

The ratio of total starch carbon released as carbon dioxide, biomass, and soluble carbon to the total carbon content of starch in the polymer composite is a measure of the percentage of the biopolymer degraded at any given time. The total carbon degraded from the starch was plotted as a function of time.

RESULTS AND DISCUSSION

Microbial Invasion

Figure 2(a) shows an electron micrograph of a fractured surface of a PE–S composite before soil burial. The composite has a 40% starch concen-

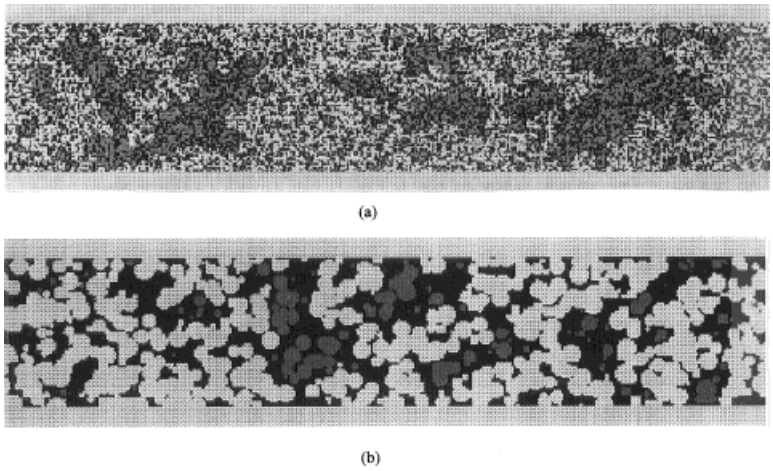

Figure 5 Effect of starch size dispersity on accessibility modeled by bilateral microbial invasion. The square 80 × 400 lattice has occupation probabilities of 61% for (a) monodisperse and (b) polydisperse PE–S composites. Connectivities are displayed for each panel.

tration by volume. The higher resolution electron micrograph in Figure 2(b) shows the starch granules of varying diameter (2–20 μm, with a typical average near 15 μm) and asymmetric shape dispersed in a PE matrix.

After soil burial, the PE–S composites exhibited color changes with fractal patterns and weight loss, indicating microbial growth and starch degradation. An increase in opacity was observed due to the starch removal by microbes.[15] A micrograph of a fracture surface of the PE–S composite after soil burial for 240 days is presented in Figure 3. It can be seen that the composite has a laced structure due to the removal of the starch by microbes. It is noticeable that the starch removal is very high, except for a few starch granules, which are not invaded by microbes. It is expected that some starch would not have been accessed because of the absence of the percolation pathways. The higher-resolution micrograph of the biodegraded thin film in Figure 3(b) also shows the colonization of microorganisms within channels and pores of the matrix that were initially occupied by starch. Spheroidal, dumbbell, and star-shaped microbes reside in the starch cavity within the polymer matrix. The nitrogen content of the composite was found to increase from 0.06 to 0.16% on soil burial for 6 months, suggesting that microbes contribute to the nitrogen content of the composite. In soil burial, the microbes and fungal hyphae invade, colonize, and discolor the composite. A similar invasion was noted in salt and fresh-water environments. These observations prompted us to propose the microbial-invasion model below.

Computer Simulation of Microbial Invasion

The starch accessibility by microbes was simulated by considering the number of microbes, microbial mobility, efficiency of conversion of starch to carbon dioxide, the lifetime of microbes, and the reproduction rate of microbes. The computer simulation of microbial invasion (one side) of a monodisperse (1-micron particles) PE–S composite at a fixed time interval for starch concentration at, above, and below p_c is shown in Figure 4(a–c). During the initial stages, the amount accessed by microbes is restricted to the near surface (a). As time elapses, the microbes access the starch percolation pathways through the PE matrix. It is clearly observable that there is a higher localized concentration of microbes in the front compared to the edge (b). The concentration of microbes in the composite is proportional to the amount of starch in the composite. The distance the microbes travel from the edge is largely controlled by the existence of starch percolating pathways. The soil burial test supports this observation, that is, the colonization of microorganisms within channels of the matrix that were initially occupied by starch [Fig. 3(b)]. As the degradation continues, the microbes invade along the percolation pathways [Fig. 4(c)].

The simulation of bilateral microbial invasion of PE–S composites with both monodisperse and polydisperse starch distribution is shown in Figure 5(a,b). A comparison of the figures clearly shows the polydispersity effect of starch grains on the starch accessibility and the resulting microstructure. For both the polydisperse and monodis-

perse composites, there are clusters of starch grains which cannot be readily accessed by microbes, because they are not present in the percolating pathway and are encapsulated by nondegradable PE.

Representative kinetic results for microbial invasion of composites with a starch fraction p of 0.57, 0.59, and 0.61 are presented in Figure 6(a–c), respectively. The microbial growth profile follows a typical S-shaped curve.[30] The curve can be divided into three phases: (I) a lag phase which is followed by a (II) growth phase and then a (III) stationary phase. The initial phase (I) is the stage where the concentration of the microorganism is constant. During the growth phase, each cell divides to produce two unit cells at a time and the microorganism's concentration increases. This is followed by a stationary phase. In Figure 6, phase I is missing, primarily because we chose starch-adapted microorganisms for simulation. The starch accessed by microorganisms up to the final stages was calculated and was found to depend on the starch concentration in the composite. For example, for a constant concentration of microbes, it was found that for a composite with $p = 0.57$ about 52% of the starch was degraded [eq. (3) predicts about 54%], while for a composite with $p = 0.61$ starch, about 84% of the starch was degraded.

In a lattice of size L^d, near p_c, the accessed fraction can be calculated from eq. (2) for a large lattice and also from the size of the fractal percolation pathway via

$$A(p) = \frac{(L/b)_{D-d}}{p} \tag{5}$$

For example, when $L = 80$, $b = 1$, $d = 2$, $p = 0.59$, and the fractal dimension $D = 7/4$, we obtain $A = 57\%$. This is less than that (84%) observed in Figures 7 and 8 because of additional surface-accessibility effects.

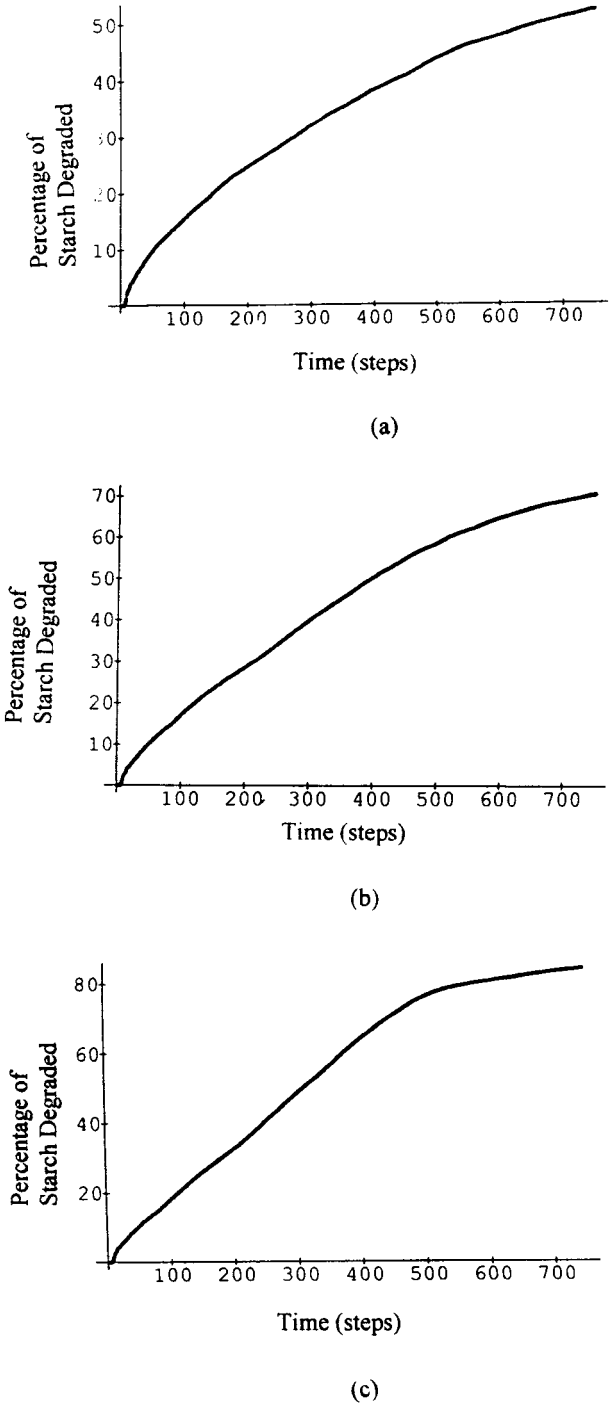

Figure 6 Simulated microbial invasion kinetics data of percent degraded starch versus time for a PE–S composite where the starch concentration is (a) 57%, (b) 59%, and (c) 61%.

Computer Simulation of Enzyme Diffusion

Bilateral enzymatic diffusion was simulated on a two-dimensional lattice using mono- and poly-dispersed PE–S composites. The enzyme release rate, enzyme diffusion coefficient, and diffusion coefficient of the product (glucose) were monitored. Amylase enzyme was chosen for the purpose of the simulation. The computer-simulation results of bilateral enzymatic diffusion of a monodisperse (starch size 1 micron) PE–S composite (with starch concentration near and above p_c) at final stages is shown in Figure 7(a,b). For samples with a starch content above p_c, there is an interconnecting starch network. With time, the enzymes percolate through the starch clusters. Due to diffusion, a gradient of enzymatic concentra-

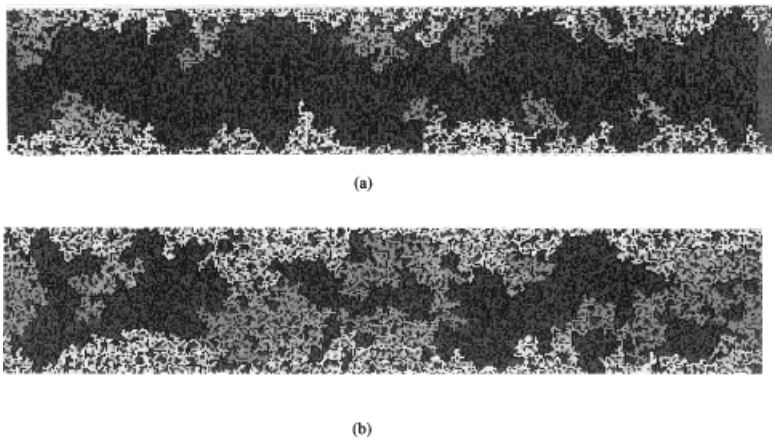

Figure 7 Effect of concentration on accessibility modeled by bilateral enzymatic diffusion. The square 80 × 400 lattice has occupation probabilities of (a) 57% and (b) 61% for a monodisperse PE–S composite. Connectivities are displayed for each panel.

tion and degraded product is noticed as the simulated sample is scanned from the edge to the center.

Representative results for enzymatic diffusion of composites with a starch fraction $p = 0.57$, 0.59, and 0.61 are presented in Figure 8. As the concentration of starch increases from 0.57 to 0.61, the slope of the curve increases sharply above p_c. Above p_c, an infinite cluster is formed. For example, for a constant concentration of enzymes at long times (1400 steps in Fig. 8), it was found that for a composite with $p = 0.57$ starch 42% of the overall starch was degraded [eq. (3) predicts about 54%], while for a composite with $p = 0.61$ starch, about 82% of the starch was degraded.

Dynamic Power-Law Exponents

Typically, the accessible fraction $A(t)$ for the data shown in Figures 6 and 8 can be expressed by a power law, $A(t) \sim t^n$, or

$$A(t) = Kt^n \tag{6}$$

where t is the time; K, a constant; and n, an exponent over some range of time t. The average time exponent n has values in the range 0 to 5/4, depending on p, and the process involved in the starch degradation.[3,24] The simulated time exponents for both microbial invasion and enzyme diffusion conditions are summarized in Table I. The *initial* slopes were measured using the initial 6% of the data; the *major* slope was obtained from the final 80% of the data and is more representative of the majority of the data.

The exponents in Table I can be understood from the following analysis: When time-dependent invasion or diffusion occurs on fractal paths with dimension D, to an average depth x, the accessed fraction of the sample of thickness L is given by[22]

$$A = x^{(D-d+1)}/L \tag{7}$$

where $x < \xi$, the correlation length. The degradation front of length N_f (shown, e.g., in Fig. 4) is related to x by

$$N_f \sim x^D \tag{8}$$

where D is the fractal dimension of the front. A lattice of width L contains $(L/\xi)^{d-1}$ independent boxes of size x^d, and, hence, eq. (7) is derived. When the accessed depth x exceeds the correlation length, a steady state is achieved and N_f becomes relatively constant. This issue was also discussed by Family et al.[31,32] with emphasis on the dynamic scaling of growing surfaces and interfaces.

As the growth front evolves, its roughness increases until it reaches a steady state. The time dependence of x is given by

$$x(t) = \alpha_0 t^\beta \tag{9}$$

in which α_0 and β are constants. For simple invasion, we expect $\beta = 1$; for diffusion, $\beta = 1/2$. The front factor α_0 should behave as $\alpha_0 \sim p$ when $p < pc$. Combining the latter two equations, we obtain the time dependence of the accessibility as

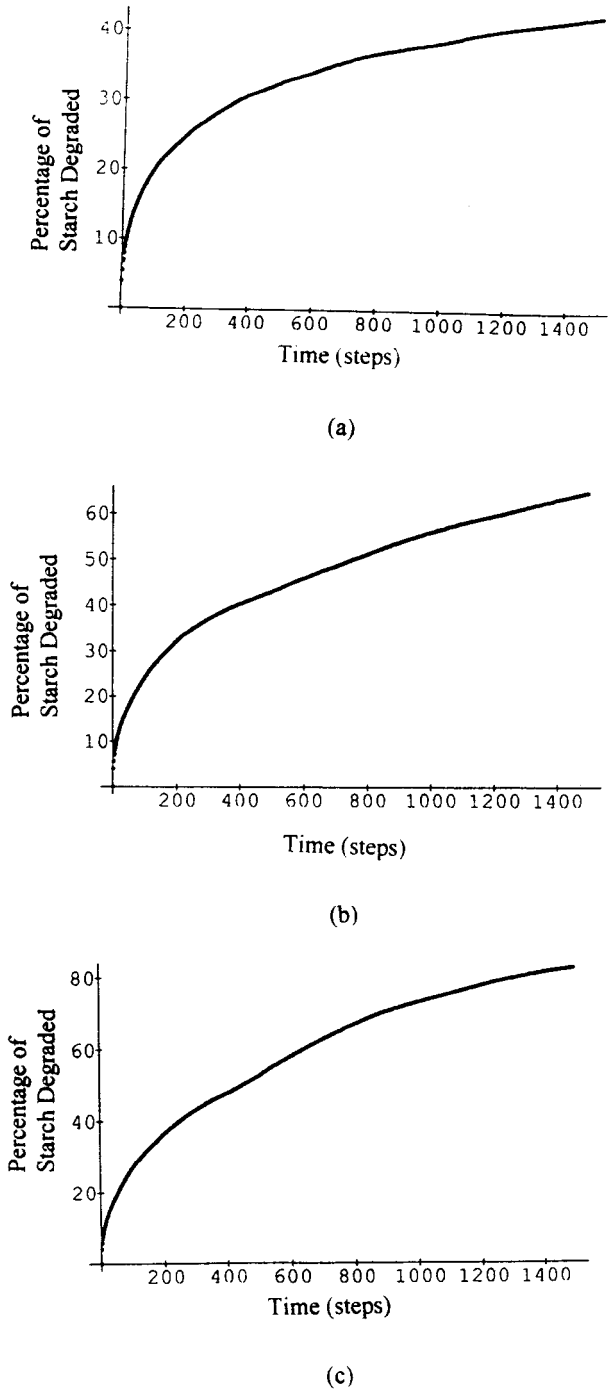

Figure 8 Simulated enzymatic diffusion kinetics data for a PE–S composite where starch concentration is (a) 57%, (b) 59%, and (c) 61%.

$$A(t) = \alpha t^n/L \tag{10}$$

where the exponent n is

$$n = \beta(D - d + 1) \tag{11}$$

in which $\beta = 1$ or 1/2, and the front factor α is

$$\alpha = \alpha_0^{(D-d+1)} \tag{12a}$$

Table II gives the theoretical exponents n, based on eq. (11), for microbial invasion ($\beta = 1$) and enzyme diffusion ($\beta = 1/2$) for two and three dimensions and fractal dimensions of percolation clusters at, above, and below the percolation threshold. The fractal dimension in each case increases with p until $D = d$ at $p = 1$. The initial exponents are essentially independent of p since the fractal pathways have not yet been developed and the starch is immediately accessible on the surface. Thus, the initial slope largely reflects the intrinsic behavior $A \sim t^\beta$.

The major kinetic exponent n is dominated by the fractal dimension existing near p_c. For the polydisperse samples, a fractal dimension of $D = 1.59$ better describes the data for both invasion and diffusion compared to $D \sim 1.8$ for the monodisperse samples. The difference in fractal dimension is due to the coarseness of the polydisperse pathways (average diameter 10 mm) compared to the monodisperse composite (diameter = 1 mm). In general, the theoretical exponents in Table II are in reasonable agreement with the simulation exponents in Table I.

Aerobic Biodegradation

Figure 9(a–c) shows the plot of the percentage of starch degraded $A(t)$ as a function of time for samples exposed to the aerobic bioreactor environment. The samples in Figure 9 had starch fractions $p = 0.2$ (a), 0.35 (b), and 0.5 (c), respectively. Below the percolation threshold [Fig. 8(a)], the accessed starch fraction f can be quantitatively determined using eq. (2). Consider, for example, a composite containing 20% by volume starch, where $p_c = 0.3117$, $p = 0.2$, $d = 3$, $b = 15$ microns, and $h = 120$ microns. Substituting the latter values in eq. (3), we obtain the surface fraction accessed as $f = 7.5\%$ of carbon accessed, which is in excellent agreement with Figure 9(a) at long times (20 days).

At $p < p_c$, the kinetic exponent n is given from the above analysis as $n = \beta(D - d + 1)$. The experimental data in Figure 8(a) can be well approximated by

$$A(t) = 1.3t^{0.6}\%/\text{min} \qquad (t < 25 \text{ min}) \tag{12b}$$

Since $d = 3$, and the fractal dimension of the clusters is approximately $D \sim 2.5$, the experi-

Table I Computer Simulation and Experimental Dynamic Exponents

			Exponent n				
Mechanism	Dispersity	Slope	57%	58%	59%	60%	61%
Microbial invasion	Mono	Initial	1.0	1.0	1.0	1.0	1.0
		Major	0.68	0.71	0.77	0.81	0.85
Accessed starch $A(p)$ %	Mono		52	57	71	79	84
Microbial invasion	Poly	Initial	1.22	1.22	1.22	1.22	1.22
		Major	0.51	0.56	0.59	0.59	0.66
Accessed starch $A(p)$% invasion	Poly		62	70	75	82	86
Enzyme diffusion	Mono	Initial	0.39	0.41	0.43	0.43	0.44
		Major	0.25	0.25	0.43	0.43	0.44
Accessed starch $A(p)$% diffusion	Mono		42	50	64	76	82
Enzyme diffusion	Poly	Initial	0.55	0.56	0.48	0.57	0.57
		Major	0.24	0.27	0.29	0.32	0.32
Accessed starch $A(p)$% diffusion	Poly		60	68	71	79	83
Biometer Results	Poly	Initial	—	—	1.39	—	0.82
		Final	—	—	0.93	—	1.57
		Average	—	—	1.16	—	1.12

mental exponent of $n \sim 0.6$ suggests that $\beta \sim 1$ and, therefore, the microbial degradation process was dominated by invasion ($\beta = 1$) rather than by enzyme diffusion ($\beta = 1/2$). A fractal dimension of 2.6 gives the exact experimental exponent $n = 0.6$, when $\beta = 1$.

Above the percolation threshold, the degradation is more extensive as the percolation pathways become accessed by microbes and enzymes, as shown in Figures 1 and 9(b,c). When $p = 0.35$, eq. (1) predicts that the final accessed fraction $A(0.35) = (0.35 - 0.3117)^{0/41}/0.35 = 75\%$, which is in good agreement with the data in Figure 9(b). Here, the initial kinetic slope is obtained as $n = 0.82$, which approaches 1.0 as the degradation proceeds. With increasing starch concentration $p = 0.5$, the final fraction of starch removed is essentially complete, $A \sim 100\%$, and the kinetic slope is of order unity, consistent with microbial invasion on a fractal structure whose dimension is approaching the embedding dimension $d = 3$.

During the initial stages of biodegradation (1–5 days), the amount of starch accessed by microbes is limited and it is restricted to the near surface. As the degradation of starch progresses, there is an increase in the microbial population to a maximum. On attaining the stationary phase, the microbes start lysing and carbon dioxide evolution continues. For example, in Figures 9(b) and 9(c), the stationary phase is approximately 10 days. As p increases from 0.35 to 0.5, the amount of starch removed at 10 days increases from 25% to about 50%. As p goes to unity, the time required to degrade the pure starch particles under similar aerobic conditions is about 5–6 days.[29]

In the kinetic equation, $A(t) = Kt^n$, both K and n depend on p in a somewhat complex manner.

Table II Theoretical and Simulated Kinetic Exponents

Mechanism	Dimension d	Fractal Dimension D	Exponent n
Invasion			
$\beta = 1$			
$P = 1$	2	2	1.0
$p \sim p_c$	2	1.89	0.89
$p < p_c$	2	1.56	0.56
Diffusion			
$\beta = 1/2$			
$P = 1$	2	2	0.5
$p \sim p_c$	2	1.89	0.45
$p < p_c$	2	1.56	0.28
Invasion			
$\beta = 1$			
$p = 1$	3	3	1.0
$p \sim p_c$	3	2.5	0.5
Diffusion			
$\beta = 1/2$			
$p = 1$	3	3	0.5
$p \sim p_c$	3	2.5	0.25

The following simplification can be useful in providing an empirical analysis of the biodegradation data: The half-life $t_{1/2}$ of the degradation process at $A(p) = 50\%$ decreases from about 14 days at $p = 0.35$ to about 11 days at $p = 0.5$, and, finally, to about 2 days at $p = 1.0$. This is approximately a linear relation with p which can be described by

$$t_{1/2}(p) \approx t^0_{1/2} - mp \qquad (p \geq p_c) \tag{13}$$

where the slope $m \sim 18$ days and the intercept $t^0_{1/2} \sim 20$ days. Combining the latter equation with eq. (10), a useful expression to describe the kinetics of biodegradation is

$$A(t, p) = 0.5[t/t_{1/2}(p)]^n \tag{14}$$

where $p \geq p_c$ and n is determined by the fractal dimension D and the invasion mechanism β via eq. (9).

CONCLUSIONS

The biodegradation of PE–S composites was investigated by considering microbial-invasion and enzymatic-diffusion mechanisms. The results show that the accessibility is dependent on the starch concentration in the composite, the distribution of starch particles in the film, the fractal microstructure, the degradation time, and the biological process by which microorganisms degrade the starch in the composite. The simulation

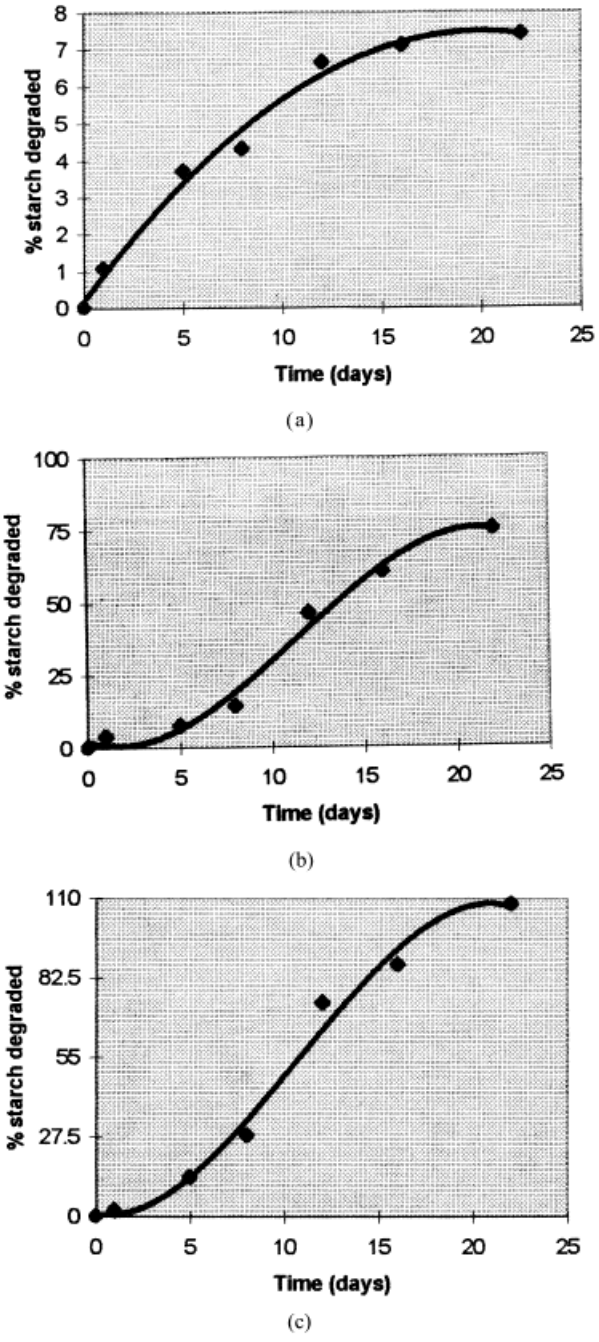

Figure 9 Biometer results of PE–S composite (a) at $p = 0.2$, (b) $p = 0.35$, and (c) $p = 0.5$. As the concentration of starch increases near the percolation threshold $p_c = 0.31$, degradation of the composite increases.

and aerobic biometer results indicate that the starch is predominantly accessed by microbes. Our soil burial studies affirm the degradation mechanism in the PE–S composite. This is based on the observation of fracture surfaces of a soil-degraded PE–S composite.

Our experimentally generated time exponents were in general agreement with the theoretical and computer-simulated data. Prior to the generalization of simulated and experimentally generated data for PE–S composites, a three-dimensional simulation is worth investigating. The modeling of the biodegradation mechanism of the PE–S composite is an important problem as is the determination of the biodegradation of PE, which is currently under evaluation. The dynamics of biodegradation should be refined to include the widest distribution of microbial species relevant to polymer and starch degradation.

The authors thank the National Science Foundation (DMR Grant 9596-267), the State of Illinois—Office of Solid Waste Research organization, and the IBM Corp. for funding this project. SEM micrographs were taken at the Center for Electron Microscopy, University of Illinois, Urbana. The elemental analyses were performed at the Center for Microanalysis, School of Chemical Sciences, University of Illinois, Urbana. The authors also thank the contributions of J. Peanasky and S. Goheen in preparing the PE–S composites and conducting the soil degradation experiments.

REFERENCES

1. Wool, R. P.; Peanasky, J.; Long, J. M.; Goheen, S. M. In Proceedings of the First International Scientific Consensus Workshop on Degradable Plastics, Toronto, 1989.
2. Wool, R. P.; Goheen, S. M. In First International Biodegradable Plastics Society Meeting, Tokyo, 1990.
3. Wool, R. P.; Raghavan, D.; Billieiux, S.; Wagner, G. C. In Second International Scientific Workshop on Degradable Polymers and Plastics, Montpellier, France, 1991.
4. Wool, R. P. In Proceedings of Biodegradable Plastics and Polymers, Osaka, Japan, 1993, Doi, Y.; Fukada, K., Eds.; Elsevier: Amsterdam, 1994.
5. Wool, R. P.; Cole, M. A. In Engineered Materials Handbook; ASM International: Ohio, 1988; p 783–788.
6. Albertsson, A. C.; Karlsson, S. J Appl Polym Sci 1988, 35, 1289.
7. Albertsson, A. C.; Karlsson, S. Polym Mater Eng 1988, 58, 65.
8. Potts, J. E. Encycl Chem Technol 1978, 4, 626.
9. Griffin, G. L. In Proceedings of Golden Jubilee Conference on Polyethylene 1933–1983; Plastics and Rubber Institute: London, 1983.
10. Otey, F. H.; Westhoff, R. P.; Doane, W. M. Ind Eng Chem Res 1987, 26, 1659.
11. Holmes, P. A. Phys Technol 1985, 16, 32.
12. Peanasky, J.; Long, J.; Wool, R. P. J Polym Sci Polym Phys 1991, 29, 565.
13. Dolezel, B. Brit Plast 1967, 49, 105.
14. Potts, J. E.; Glendinning, R. A.; Ackart, W. B.; Niegisch, W. D. Polymers and Ecological Problems; Guillet, J. E., Ed.; Plenum: New York, 1973; pp 61–80.
15. Goheen, S. M.; Wool, R. P. J Appl Polym Sci 1991, 42, 2691.
16. Stauffer, D. Introduction to Percolation Theory; Taylor and Francis: London, 1985.
17. Broadbent, J. M.; Hammersley, S. R. Proc Camb Philos Soc 1957, 53, 629.
18. Flory, P. J. Principles of Polymer Chemistry; Cornell University: Ithaca, NY, 1953; Chapter 9.
19. Stauffer, D.; Congolio, A.; Adam, M. Adv Polym Sci 1982, 44, 103.
20. Sapoval, B.; Rosso, M.; Gouyet, J.-F. J Phys Lett 1985, 46, L149.
21. Kantor, Y.; Webman, I. Phys Rev Lett 1984, 52, 1891.
22. Wool, R. P. Polymer Interfaces: Structure and Strength; Hanser: Munich, 1995.
23. Wool, R. P. In Proceedings of the World Congress on Adhesion, WCARP-1, Garmish-Partenkichen, Germany, 1998.
24. Wool, R. P. In Degradable Polymers, Scott, G.; Gilead, D., Eds.; Chapman & Hall: London, 1995; Chapter 7, pp 138–152.
25. Neidhart, F.; Ingraham, J.; Schaechter, M. Physiology of the Bacterial Cell; Sinauer: USA, 1990.
26. Peanasky, J. M.S. Thesis, University of Illinois, Urbana, 1990.
27. Raghavan, D.; Wagner, G. C.; Wool, R. P. Polym Mater Sci Eng 1992, 67, 357.
28. Gunsalus, I. C.; Wagner, G. C. Methods Enzymol 1978, 52, 166–188 (modified unpublished G. C. Wagner).
29. Raghavan, D.; Wagner, G. C.; Wool, R. P. J Environ Degrad Plast 1993, 1, 203.
30. Deacon, J. W. In Basic Microbiology; Wilkinson, J. F., Ed.; Blackwell: London, 1986; pp 42–46.
31. Dynamics of Fractal Surfaces; Family, F.; Vicsek, T., Eds.; World: Singapore, 1991.
32. Fractal Aspects of Materials; Family, F.; Meakin, P.; Sapoval, B.; Wool, R. P., Eds.; Materials Research Society Symposium Proceedings, Dec. 1994; Vol. 367.